



Zoologischer Anzeiger

Volume **306** 2023

A Journal of Comparative Zoology





Contents lists available at ScienceDirect

Zoologischer Anzeiger

journal homepage: www.elsevier.com/locate/jcz

A landmark-based geometric morphometric approach to quantify deviations from bilateral symmetry in polyplacophorans

Brenda Paola Ramirez-Santana^{a,b}, Sandra Milena Ospina-Garcés^{c,d,*},
Jorge Saul Ramirez-Perez^a, Omar Hernando Avila-Poveda^{a,b,e,**}

^a Facultad de Ciencias del Mar (FACIMAR), Universidad Autónoma de Sinaloa (UAS), Mazatlán, Sinaloa, México

^b Proyecto Quitón del Pacífico tropical mexicano. Mazatlán, Sinaloa, México

^c Centro de Investigación en Biodiversidad y Conservación (CIByC), Universidad Autónoma del Estado de Morelos, Cuernavaca, Morelos, México

^d Centro de Investigaciones Tropicales (CITRO), Universidad Veracruzana (UV), Xalapa, Veracruz, México

^e Programa de Investigadoras e Investigadores por México, Consejo Nacional de Humanidades, Ciencias y Tecnologías (CONAHCYT), Ciudad de México, México

ARTICLE INFO

Handling Editor: Carsten Lueter

Keywords:

Left-right asymmetry
Scleritome
Teratology
Fluctuating asymmetry
Mollusca

ABSTRACT

The class Polyplacophora (chitons) represents a dorsoventrally flattened mollusk group that has an oval-shaped body covered with eight overlapping sclerites providing bilateral symmetry. Chitons show abnormalities (teratologies) that are characterized by symmetry deviations between the right and left sides of their bodies. As these deviations do not result in damage that affects vital functions, chitons are able to reach adult stages. In this study, we quantify the asymmetric condition of the species *Chiton articulatus* using a landmark-based geometric morphometric approach to assess variation in shape and bilateral symmetry. A geometric configuration of 22 landmarks and 50 semi-landmarks was created to evaluate shape variation in abnormal and deformed specimens compared to normal *Chiton articulatus* specimens. Vectors of change in the body shape configurations of chitons indicate that the greatest change occurs in the anterior part of the body, with less change in the middle and posterior parts. This gives chitons a widened appearance and provides anatomic compensation to restore the bilateral symmetry of the body scleritome. The diverse abnormalities and deformities had little impact on shape variations and confirmed that the coalescence condition is an intermediate step between a normal condition and the abnormal conditions of hypomerism or hypermerism. The low levels of fluctuating asymmetry expressed in *C. articulatus* indicate that despite living in areas of high stress, such as the rocky intertidal coast, this species maintains stability in its development and shape. Our results can serve as a model for studying bilateral symmetry deviation in polyplacophorans.

1. Introduction

Bilateral symmetry is the simplest type of symmetry in biological systems (Savriama 2018). The left and right sides of an organism with bilateral symmetry have a gene configuration that expresses the same shape on each side (Palmer 1994; Finnerty et al. 2004), making the left and right sides appear as mirror images in the sagittal plane of the body plan (Holló 2015). Bilateral symmetry is maintained regardless of the position and orientation of the body plan (Palmer 1994; Manuel 2009). In Bilateria, at least three types of symmetry deviations characterize the body plan (Palmer 1994): directional asymmetry, antisymmetry, and

fluctuating asymmetry (Klingenberg 2015; Scalici et al. 2017), with fluctuating asymmetry being the most frequent type. Fluctuating asymmetry involves variation between the left and right sides caused by small disturbances that occur during embryological development that accumulate and are expressed on one side of the body plan (Dongen 2006; Gutiérrez-Cabrera et al., 2022; Klingenberg 2022). Although this asymmetric condition can cause an abnormal shape (i.e., small differences between the right and left sides) due to random developmental processes, fluctuating asymmetry does not cause functional damage in organisms in which it occurs (Benítez et al. 2020) and has a statistic distribution of about an R – L mean of zero compared to other types of

* Corresponding author. Centro de Investigación en Biodiversidad y Conservación (CIByC), Universidad Autónoma del Estado de Morelos, Cuernavaca, Morelos, México.

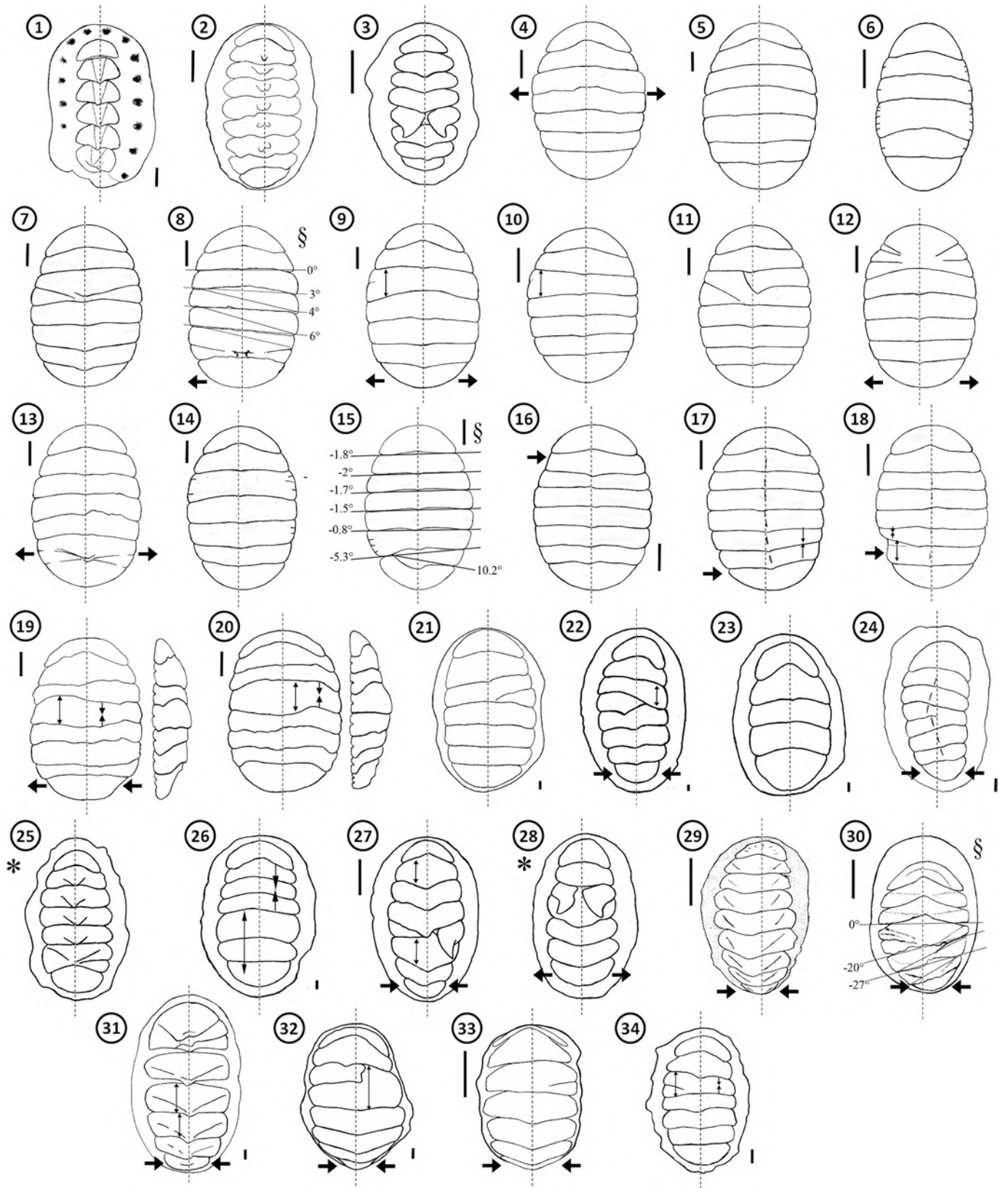
** Corresponding author. Facultad de Ciencias del Mar (FACIMAR), Universidad Autónoma de Sinaloa (UAS), Mazatlán, Sinaloa, Mexico.
E-mail addresses: sandra.ospina@uaem.edu.mx (S.M. Ospina-Garcés), oavila@uas.edu.mx, ohavilapo@conahcyt.mx (O.H. Avila-Poveda).

<https://doi.org/10.1016/j.jcz.2023.06.008>

Received 25 February 2023; Received in revised form 5 June 2023; Accepted 27 June 2023

Available online 4 July 2023

0044-5231/© 2023 Elsevier GmbH. All rights reserved.



(caption on next page)

Fig. 1. Schematic drawings of abnormal chitons exhibiting bilateral asymmetry in the scleritome outline. 1. *Acanthochiton rubrolineatus*, 8 mm TL (Taki, 1932); 2. *Acanthopleura gemmata*, 52 mm TL (Dell'Angelo & Schwabe, 2010); 3. *Acanthopleura granulata*, 35 mm TL (Kingston et al. 2020); 4. *Chiton articulatus*, 54 mm SL (Avila-Poveda et al. 2019); 5. *C. articulatus*, 61.5 mm SL (Avila-Poveda et al. 2019); 6. *C. articulatus*, 33 mm SL (this study); 7. *C. articulatus*, 53.3 mm SL (Avila-Poveda et al. 2019); 8. *C. articulatus*, 54 mm SL (this study); 9. *C. articulatus*, 64 mm SL (Avila-Poveda et al. 2019); 10. *C. articulatus*, 37.5 mm SL (Avila-Poveda et al. 2019); 11. *C. articulatus*, 52 mm SL (Avila-Poveda et al. 2019); 12. *C. articulatus*, 45.6 mm SL (Avila-Poveda et al. 2019); 13. *C. articulatus*, 61 mm SL (this study); 14. *C. articulatus*, 55 mm SL (Avila-Poveda et al. 2019); 15. *C. articulatus*, 49.1 mm SL (Avila-Poveda et al. 2019); 16. *C. articulatus*, 44.1 mm SL (this study); 17. *C. articulatus*, 40.2 mm SL (this study); 18. *C. articulatus*, 40.7 mm SL (this study); 19. *C. articulatus*, 57.6 mm SL (this study); 20. *C. articulatus*, 60.7 mm SL (this study); 21. *Chiton magnificus*, 19 mm TL (Torres et al. 2018); 22. *Chiton olivaceus*, 26 mm TL (Baschieri et al. 1992); 23. *C. olivaceus*, 16 mm TL (Dell'Angelo & Palazzi, 1983); 24. *Craspedochiton laqueatus*, 11.8 mm TL (Anseeuw & Terryn, 2003); 25. *Eudoxoplax inornata*, * (Iredale & Hull, 1925); 26. *Ischnochiton rissoi*, 22 mm TL (Baschieri et al. 1992); 27. *Liolophura japonica*, 40 mm TL (Taki 1932); 28. *Liolophura queenslandica*, * (Iredale & Hull 1925); 29. *Nutallina* sp., 33.4 TL (Berry, 1935); 30. *Placiphorella stimpsoni*, 33 mm TL (Taki, 1932); 31. *Tonicella granulata*, 17 mm TL (Dell'Angelo, 1982); 32. *Tonicella rubra*, 16.4 mm TL (Langer, 1978); 33. *Tonicia atrata*, 30.8 TL (Guillén & Urteaga, 2019); 34. *Tonicia sueziensis*, 11.9 mm (Anseeuw & Terryn, 2003). The thick black arrows indicate the direction in which the sclerite widens or narrows towards the outline of the scleritome. Thin black arrows within the sclerites indicate the direction in which the sclerite(s) widens or narrows along the anteroposterior axis of the scleritome. TL = Total length, SL = Scleritome length. TL can be obtained through an equation applicable to large size chitons in the adult stage: $TL = SL + 7 \text{ mm}$ (Avila-Poveda et al. 2020). Scale bar is 10 mm except in numbers 1, 21, 22, 23, 24, 26, 31, 32, 34, where scale bar is 1 mm * No length measurements. [‡]Abnormal chiton that may present in a malformed pattern such as helicomerism, according to Scholtz (2021). The dotted line and number indicate the degree of inclination. Each chiton was redrawn from its respective publication.

symmetry (Palmer 1994).

Polyplacophorans are mollusks with dorsoventrally flattened, oval-shaped bodies that are typically covered by eight overlapping sclerites (also called plates or valves) (Ruppert & Barnes 1996; Anderson 2001; Brusca & Brusca 2005). The sclerites create iterative units that are arranged in series (Kingston et al. 2020) along an anteroposterior axis in the scleritome (i.e., the collective set of sclerites that form the articulated shell of polyplacophorans). These units share certain inherent morphological structural properties (Scholtz 2021) and provide bilateral symmetry to the scleritome. The body shape of polyplacophorans can serve as a model by which to study abnormal expressions that deviate from bilateral symmetry.

For decades, abnormalities (teratologies) have been observed in the scleritome of various polyplacophorans (e.g., Taki 1932; Dell'Angelo & Schwabe 2010). There are several types of teratologies. These are characterised by the number of sclerites (valves or plates), either increased (hypermerism) or decreased (hypomerism); the fusion between sclerites (coalescence); and the division of sclerites (splitting) (Crozier 1919; Pelseneer 1919; Chace & Chace 1930; Berry 1935; Roth 1966; Burghardt & Burghardt 1969; Langer 1978; Dell'Angelo 1982; Dell'Angelo & Cianfanelli 2002; Anseeuw & Terryn 2003; Prelle et al. 2013; Torres et al. 2018, among many others). Recently, complex combinations of abnormalities (Avila-Poveda et al. 2019), as well as a putative spiral malformation condition called helicomerism (Scholtz 2021), have been described. At first sight, these abnormalities show an ellipsoid outline with unnoticeable asymmetry between the right and left sides of the scleritome (Fig. 1).

Abnormalities in the scleritome of chitons are caused by an uncontrolled deposition of calcium carbonate at the anterior margin of the sclerites during embryonic development prior to settlement, resulting in deformations in the scleritome contour formation pattern (Taki 1932; Kniprath 1980; Kocot et al. 2016). Whether the change occurs to a greater or lesser extent over the oval body appearance of these organisms, it apparently does not cause damage that affects their vital functions (Taki 1932) or their survival, since these changes have been observed in abnormal chitons that have reached adult stages (e.g., Avila-Poveda et al. 2019; Kingston et al. 2020). This demonstrates that “although an asymmetric condition gives an abnormal appearance in shape, fluctuating asymmetry does not represent functional damage in individuals who present it” (Benítez et al. 2020). Consequently, this fluctuating asymmetry could serve as a proxy for analysing the bilateral symmetry of normal and abnormal polyplacophorans.

The change in body shape of abnormal chitons has been analysed through classical morphometrics, using length/width ratio to describe the compensation that occurs towards elongation (Taki 1932) or width/length ratio to describe the compensation that occurs towards widening (Avila-Poveda et al. 2019). Abnormal chitons possess a widened body shape based on their width/length ratio; this ratio

increases compared to that of normal chitons and could reflect a form of an anatomic compensation intended to restore the bilateral symmetry of the body scleritome (Avila-Poveda et al. 2019). From a top-view perspective, chitons have an elliptic oval body shape that adjusts to either a broad-oval, oval, and/or elongated-oval shape (Schwabe 2010). Therefore, the height/width ratio of the intermediate valve helps to define dorsal elevation for chitons as being either low, moderate, or high (Kaas & Van Belle 1981; Schwabe 2010) and is used as a feature in the phylogenetic analysis of chitons (Sigwart et al. 2007). The length/width ratio helps to define body shape as being broad oval, oval, or elongated-oval (Schwabe 2010; Avila-Poveda 2013). A width/length ratio is sometimes used to support taxonomic morphometric descriptions (e.g., Ferreira 1983; Sampedro-M et al. 2012; Quintana & Hernández 2021) or to explore morphological differences between ecotypes and ecoregions (Sirenko & Ibañez 2023).

Landmark-based geometric morphometric features have been effectively used to characterize shape and size variation across populations in a wide diversity of Mollusca and ecological contexts (e.g., Teso et al. 2011; Dunithan et al. 2012; Tamburi & Martín, 2013; Yuvero & Giménez 2021; Doyle et al. 2022). Polyplacophorans, in particular have a body outline that is covered by the mantle girdle, which delineates an ellipse but hides access to anatomical landmarks (such as shallow notches on the lateral margins of each sclerite). Taking advantage of this oval elliptical contour, Salloum et al. (2020) delineated the mantle girdle and applied Fourier elliptic analysis (Kuhl & Giardina 1982) to measure and compare body shape variation in several populations of the chiton species *Onithochiton neglectus* and found that the northern and southern populations were separated according to their shape, which corresponds to a regionally variable ecological association that links the chiton to kelp holdfasts. On the other hand, while our manuscript was in undergoing a peer review process, a new article was published that revealed a landmark-based geometric morphometric analysis of chitons whose mantle girdle was maintained. The authors used the intersection of the sclerites as homologous points to describe the shape and size variation of the chiton *Stenoplax limaciformis* between marine ecoregions and found that although there are differences in shape among marine ecoregions, these differences are not associated with centroid size, and therefore allometry is not significant between marine ecoregions (Hernández-P et al. 2023).

Chiton articulatus is a polyplacophoran endemic to the Mexican Tropical Pacific; specimens with a complex combination of abnormalities (i.e., teratologies) have been reported (Avila-Poveda et al. 2019), and recently the authors of this paper discovered some specimens with deformities (i.e., having eight sclerites but unusual body outlines) that seem to modify the bilateral symmetry of the scleritome. Since the mantle girdle was removed from these chitons, it is possible to access the slit rays on the lateral margins of each sclerite, which serve as anatomical reference points (Taki 1932; Avila-Poveda et al. 2019).

Table 1
Types of combinations of abnormalities and deformities reported in *C. articulatus*.

Abbreviation	(Sclerite number) and type of abnormality or deformity	Amount of chitons	width/length ratio	Schematic drawing ID
HypoP	(7) perfect hypomerism	2	0.59, 0.62	Fig. 1, No. 4-5
HypoCo	(6) hypomerism combined with coalescence IV-V-VI	1	0.61	Fig. 1, No. 6
HeCo	(7) heterogeneous coalescence III-IV	1	0.59	Fig. 1, No. 7
HeCo	(7) heterogeneous coalescence VI-VII. Probable helicotomy ^a	1	0.67	Fig. 1, No. 8
HeCo	(7) heterogeneous coalescence III-IV combined with hypomerism	2	0.59, 0.64	Fig. 1, No. 9-10
HeCo	(7) heterogeneous coalescence III-IV combined with imperfect hypermerism	1	0.63	Fig. 1, No. 11
HeCo	(6) heterogeneous triple-coalescence I-II-III	1	0.67	Fig. 1, No. 12
HeCo	(6) heterogeneous triple-coalescence VI-VII-VIII	1	0.59	Fig. 1, No. 13
HoCo	(7) homogeneous coalescence III-IV combined with imperfect hypermerism	1	0.60	Fig. 1, No. 14
HoCo	(8) homogeneous triple-coalescence VI-VII combined with imperfect hypermerism. Probable helicotomy ^a	1	0.60	Fig. 1, No. 15
W	(8) apparent widening in a side of the chiton scleritome	1	0.55	Fig. 1, No. 16
S	(8) scoliosis-like torsion	1	0.56	Fig. 1, No. 17
B	(8) "bitten" one side reduced	1	0.60	Fig. 1, No. 18
H	(8) hunchbacked	2	0.50, 0.46	Fig. 1, No. 19-20
Mean ratio			0.58 ± 0.03 (n = 3405) ^b	

^a Probable helicotomy, following Scholtz (2021).

^b Refer to normal specimens with eight sclerites (Avila-Poveda, unpublished data, Proyecto Quitón del Pacífico tropical mexicano). Source of schematic drawing like Fig. 1.

Therefore, these abnormal specimens may serve as a model for analysing shape variation, using a landmark-based geometric morphometric approach to assess variation in shape and bilateral symmetry of the scleritome.

The aim of this study is to assess whether complex abnormalities in Polyplacophora generate asymmetry between the right and the left side or retain their bilateral symmetry with a normal oval body shape. Here, we present the first landmark-based protocol for quantifying the shape variation of the scleritome body outline in abnormal and deformed specimens compared to normal *Chiton articulatus* specimens. We also provide information on the direction and magnitude of the shape variation to test whether coalescence is an intermediate step between the normal condition and the conditions of hypomerism or hypermerism, as proposed by Avila-Poveda et al. (2019).

2. Material and methods

2.1. Source and handling of chitons

For this study, 396 randomly collected adult chitons were used during a monthly research project that was carried out from 2015 to the present in seven locations throughout the geographic distribution of *Chiton articulatus* in the Mexican Tropical Pacific (Avila-Poveda 2020). Of these 396 chitons, 17 had scleritome abnormalities. Table 1 describes 12 abnormal chitons (i.e., with teratologies) and 5 deformed chitons (i.e., those with eight sclerites but unusual body outlines) of *Chiton articulatus*, which were used in this study to validate the geometric morphometric protocol and assess possible asymmetry in the shape of the scleritome. All chitons were relaxed to keep their shapes as natural as possible (Avila-Poveda 2013).

To facilitate the understanding of the terms that are used here to refer to the different types of body conditions presented by chiton scleritome, we have provided some definitions based on Dell'Angelo and Schwabe (2010) and the Cambridge Dictionary:

- *normal*: refers to the ordinary chiton, which always has eight structurally well-formed sclerites that make up an oval shape in a common pattern (i.e., the body scleritome of chitons).
- *abnormal*: refers to chitons whose features differ from those of ordinary chitons with regard to the sclerites and the scleritome due to any teratology (i.e. hypermerism, hypomerism, coalescence, or splitting) and the combinations among them that modify the usual oval shape of the body scleritome.

- *deformed*: refers to a chiton that always has eight sclerites but one or more of them has developed irregularly on any of its sides, thus modifying the normal oval shape of the body scleritome.

Coalescence refers to the way in which the sclerites merge. In homogeneous coalescence, the sclerites are merged to form a single sclerite that shows no visual traces of its junction, whereas in heterogeneous coalescence, traces of merging of the sclerites is visible and implies distinguished points of junction in any part of the sclerite (Avila-Poveda et al. 2019).

A perfect or imperfect condition refers to the number of slit(s) and of slit ray(s) per side in the insertion area of each intermediate sclerite following the normal slit formula of the species, in this case *C. articulatus* [[slits formula: [13–18(I)/1(II-VII)/16–22(VIII)]]] (Ferreira 1983; Bullock 1988; Poutiers 1995); the perfect condition follows this formula, while the imperfect condition shows a different number of slits from the formula on one or more sides of any sclerite (Supplement 1).

2.2. Preparation of specimens

Anatomically, the head, intermediate, and tail sclerites have slits where the mantle girdle is inserted, covering the outline of the chiton scleritome [[slits formula: [13–18(I)/1(II-VII)/16–22(VIII)]]] (Ferreira 1983; Bullock 1988; Poutiers 1995). Therefore, before digitization, it was necessary to carefully separate the mantle girdle from scleritome to access the slits (Fig. 3 in Abadia-Chanona et al. 2016), which represent the most suitable points for the placement of landmark points (Fig. 2). Once we removed the mantle girdle, top-view perspective photographs of the dorsal part of the scleritome of the abnormal and normal chitons were taken over a white background. A three-step protocol was established. First, a CANON G5 camera was mounted on a fixed structure to avoid distortion in the periphery of the photographs, as well as to maintain the same apertures and focal distances, following the fundamentals of photography for geometric morphometric analysis (Zelditch & Swiderski 2021). Second, each chiton was oriented horizontally with the head sclerite to the left and positioned at the centre of the photograph. Third, two guides with scales were placed: the first 1 cm long near the chiton, in the coplanar height, and the second a ruler in the lower part of the visual field of the camera lens to enable subsequent rescaling of the images.

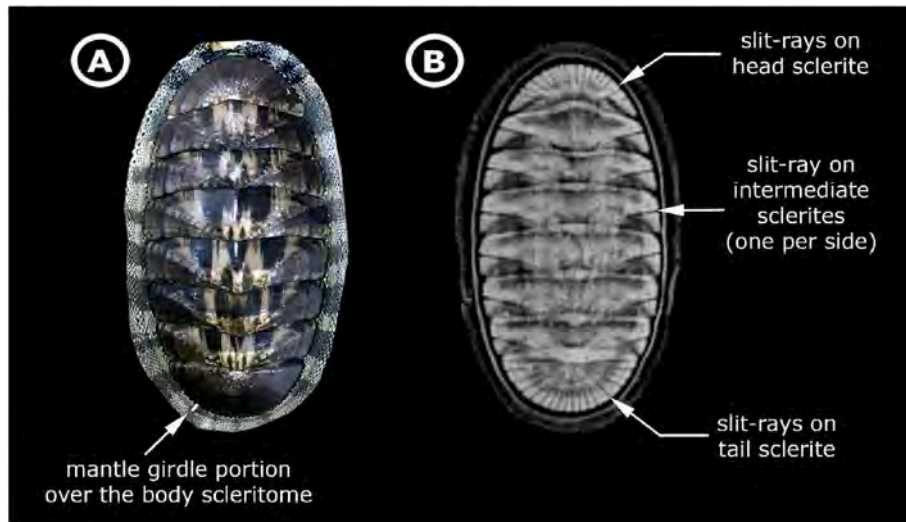


Fig. 2. Dorsal view of the scleritome of *Chiton articulatus*. A) Photograph of the scleritome with the mantle girdle covering the sclerites. B) X-ray of a chiton showing slit-rays below the mantle. Slits formula for *C. articulatus*: [13–18(I)/1(II–VII)/16–22(VIII)] (Ferreira 1983; Bullock 1988; Poutiers 1995).

2.3. Geometric morphometric data

Shape analysis based on anatomical landmarks is the most common and useful approach in geometric morphometrics for appropriately capturing and quantifying variation and deviations in shape and size (Rohlf & Slice 1990; Bookstein, 1996; Adams et al. 2004; Zelditch & Swiderski, 2021). Therefore, we designed a two-dimensional landmark protocol to quantify deviations from symmetry in polyplacophorans with abnormal and deformed body scleritome shapes.

Photographs were ordered and grouped in a single digitalization file for morphometric analysis using the free software TpsUtil. To locate landmarks and semi-landmarks, we considered Bookstein (1996) criteria. Here, we took as anatomical landmarks the intersections between the sclerites as well as the single slit on the left and right side of each intermediate sclerite. A total of 5 landmarks were placed between sclerite intersections and 6 landmarks in the slit rays of the sclerites on each side of the scleritome, giving a total of 22 landmarks. Concerning anatomical semi-landmarks, a line of 25 equidistant points was configured and placed around the curvature of the head and tail sclerites. This number of points was selected based on the maximum number of slit rays that can be found in the head and tail sclerite of each organism or species (i.e., slit formula), as they recover contour variations well (Fig. 3). The placement of landmarks and semi-landmarks was conducted using the free software TPSdig 2.3 (Rohlf 2017). Since polyplacophorans have bilateral symmetry, and to avoid attributing changes in shape to a digitalization error, the total sample was digitalized twice, and a Procrustes ANOVA was performed to calculate the digitalization error.

To ensure that the set of photographs contained the same number of landmarks and semi-landmarks per chiton, and to consider normal, hypermerism, and hypomerism conditions, we set two context: 1) each intermediate sclerite had at least one slit ray per side, and 2) in chitons with coalescence and perfect hypomerism, the landmarks were placed in the widest sclerite (Fig. 3), given the knowledge that the width/length ratios of individual sclerites increase with abnormalities (Ferreira 1983; Ibañez et al. 2018; Salloum et al. 2023). A generalized Procrustes analysis (GPA) was performed using R software (R Core Team 2017) to rule out morphological elements that did not contribute to shape. Semi-landmarks were aligned using the “bending energy” method (Bookstein 1996), which optimizes the location of semi-landmarks, minimizing the deformation energy concerning a consensus curve (Gunz & Mitteroecker 2013). Additionally, we obtained a size estimator for each chiton configuration, called Centroid Size (CS), calculated as

the squared sum of each landmark to the centroid coordinates (Zelditch & Swiderski, 2021). Both shape, represented by aligned configurations, and size variables were statistically analysed to test deviations from bilateral symmetry.

2.4. Exploratory analysis and statistical analysis

All the exploratory analyses and statistical comparisons below were performed using Geomorph 4.0.3 (Adams et al. 2019), RRPP 0.6.1 library (Collyer & Adams 2018, 2019), and R software (R Core Team 2017).

2.4.1. Body shape variation (using PCA)

A principal component analysis (PCA) was performed to describe shape variance between normal and abnormal chitons. Since the abnormal specimens in this study are a limited sample of individuals (Table 1), they were treated and grouped in the PCA according to whether they had heterogeneous or homogeneous coalescence. In addition, the conditions of HoCo (homogeneous coalescence), HypoCo (hypomerism), and HypoP (perfect hypomerism) were considered as a single group called Hypo-HoCo, based on our hypothesis that homogeneous coalescence is an intermediate step toward perfect hypomerism or perfect hypermerism, with a very low change effect among them compared to the condition of heterogeneous coalescence (Avila-Poveda et al. 2019).

Deformation grids from the consensus shape, on the extremes of variance axis (first two principal components), were used to identify changes in body shape in abnormal individuals.

2.4.2. Bilateral symmetry test and FA component

To assess the effect of teratologies on the left and right sides, we performed a bilateral symmetry test and obtained the fluctuating asymmetry (FA) component of body shape variance to evaluate differences in levels of asymmetry between normal and abnormal conditions in chitons. The levels of FA asymmetry between normal and abnormal chitons could be compared and quantified according to overall mean asymmetry; that is, levels of directional asymmetry in the total sample were evaluated as defined by Klingenberg (2015). The symmetry test shows variation due to the interaction between individual and body side (Adams & Otárola-Castillo 2013). We then evaluated shape differences between normal (symmetric) and abnormal (asymmetric) individuals, as a single group due the low group size in types of abnormalities using a Procrustes ANOVA model.

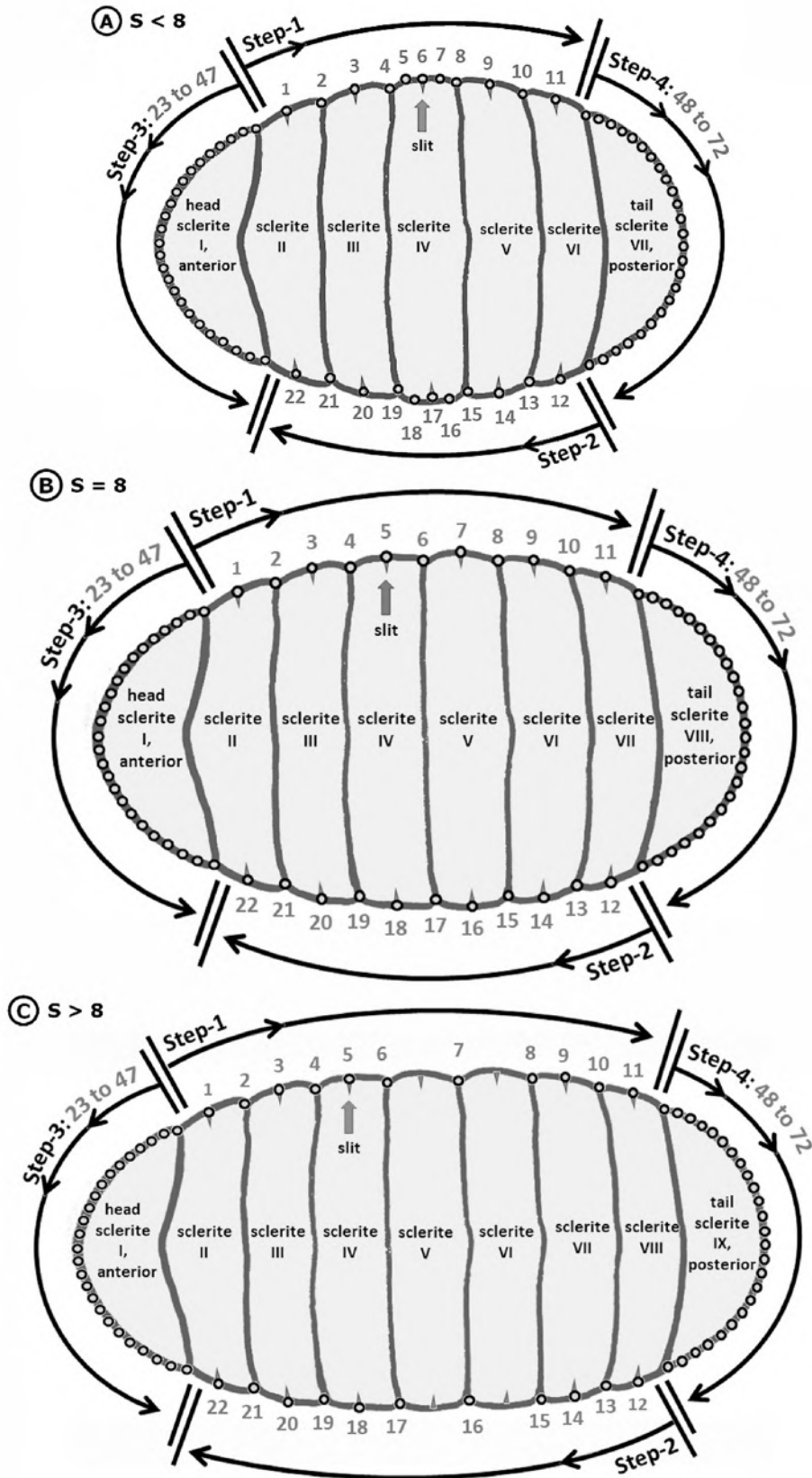


Fig. 3. Infographic of landmarks and semi-landmarks (dots) of the *Chiton articulatus* scleritome (i.e., the collective of sclerites “S” without mantle girdle) in dorsal view. The exposure of the slit in the dorsal view of each intermediate sclerite is figurative of its actual position in the ventral view. A) represents hypomerism condition, B) represents normal condition, and C) represents hypermerism condition.

Table 2

Set and location of landmarks and semi-landmarks over the scleritome used to analyze the shape and symmetry of polyplacophorans.

Structure	Landmarks – Semilandmarks	Anatomical location
Scleritome	1,3,5,7,9,11,13,15,17,19,21	Intersection between sclerites
	2,4,6,8,10,12,14,16,18,20,22	The midline of muscle attachment to the sclerite, Slit-ray formula for the species <i>C. articulatus</i> : 13–18(I)/1(II-VII)/16–22(VIII)
	23: 47	Head sclerite curvature
	48: 72	Tail sclerite curvature

2.4.3. Vectors used to describe shape variation of abnormal and deformed chitons

The average configuration of replicates was used to describe shape differences between abnormal conditions. The direction and magnitude of the changes in the body shape of abnormal and deformed (Def) chitons were contrasted against a sample of normal chitons to estimate a consensus shape. Abnormal chitons were grouped according to the complex abnormality combinations: perfect hypomerism (HypoP); hypomerism and coalescence (HypoCo); heterogeneous coalescence (HeCo), when traces of the junction are visible; and homogeneous coalescence (HoCo), when the junction forms a single whole sclerite with no visual traces of its junction.

2.4.4. Shape comparisons between normal and abnormal conditions

The entire shape configuration of individuals (the average between replicates) was analysed to describe shape and size variance between abnormal and normal conditions, using Procrustes ANOVA and ordinary linear models, respectively. We tested the percentage of shape variance explained by CS, abnormal or normal condition, and their interaction. We described trends of shape change with each increment of size within each group of abnormalities using a least squares regression line and compared allometric vectors between these groups of abnormalities. The significance of each variable in the statistical model was assigned by a permutation procedure on the residuals of the model, through 1000 replicates. The groups that were compared were the same as those used

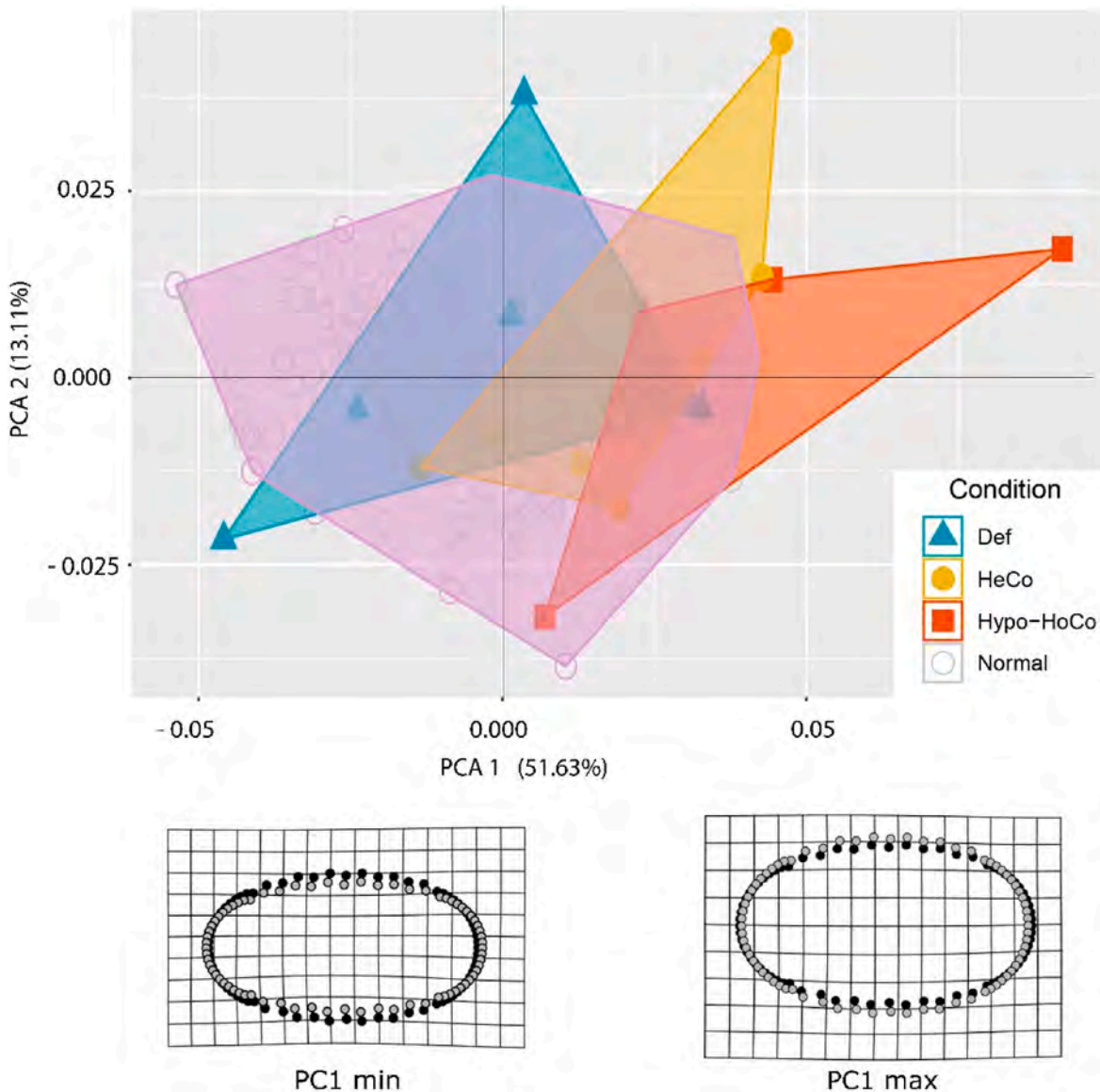


Fig. 4. Morphospace described by the first two principal components showing the position of individuals from different conditions (symbol). Deformation grids are presented, indicating the direction of minimum and maximum shape change.

Table 3

Bilateral symmetry test to calculate fluctuating asymmetry (FA) component of body shape variance. The R squared values (Rsqr) give an estimate of the contribution of each factor to the total shape variation.

	Df	SS	MS	Rsqr	F	Z	Pr(>F)
Ind	395	0.71757	0.0018166	0.60382	4.3065	19.5259	0.001 ^a
Side	1	0.02019	0.0201858	0.01699	47.8523	5.0322	0.001 ^a
ind:side	395	0.16663	0.0004218	0.14021	1.1764	3.7113	0.002 ^a
ind:side:replicate	792	0.28400	0.0003586	0.23898			
Total	1583	1.18839					

^a Significant effect alpha <0.01.

Table 4

Results from the Procrustes ANOVA model to evaluate the effect of condition (abnormal and normal) on the observed FA shape variation.

	Df	SS	MS	Rsqr	F	Z	Pr (>F)
Condition	1	0.0006	0.0006	0.0027	1.0673	0.5245	0.31
Residuals	394	0.2331	0.0005	0.9973			
Total	395	0.2337					

**Significant effect alpha <0.01.

in the PCA space, and we considered groups with more than two specimens. We also evaluated shape differences between groups using pairwise Procrustes distances between group means. The significance of distances was tested via a permutation procedure with 1000 replicates using Morpho ver. 2.7 (Schlager et al. 2019).

3. RESULTS

3.1. Landmark protocol validation and digitalization error

A final configuration of 22 landmarks and 50 semi-landmarks was set (Table 2) to effectively describe the body shape of the chitons. The specimens were mainly placed in a clockwise direction, following 4 steps: Step 1, starting at the top of the photograph from left to right; Step

2, starting at the bottom from right to left; Step 3, on the head sclerite from top to bottom; and Step 4, on the tail sclerite also from top to bottom (Fig. 3). This configuration can be used for chitons with hypomerism (less than eight sclerites, Fig. 3A), normal condition (eight sclerites, Fig. 3B), or hypermerism (more than eight sclerites, Fig. 3C). The digitalization error accounts for 0.28% of total shape variation ($F_{1,791}=2.212$, $P = 0.076$), while 99% of total shape variation can be explained by biological variations in the condition of the chiton scleritome.

3.2. Variation in body shape

The first two main components indicated changes in the shape of the chiton scleritome, representing a 64.74% shape variation, with abnormal (HeCo and Hypo-HoCo) and deformed (Def) groups overlapping to normal, perhaps with Hypo-HoCo specimens having wider ranges (Fig. 4). On the axis of the PC1, deformation grids were observed in the contour of the scleritome (landmarks 1:11, 12:22); the group of normal chitons showed the greatest vector changes towards the negative direction of the axis and the rest of the abnormalities were towards the positive direction of the axis. For the PC2, a greater dispersion was observed in the groups that were deformed (Def) and had heterogeneous coalescence (HeCo). The deformation grids indicated that the largest changes in shape occurred over the width of the scleritome (landmarks

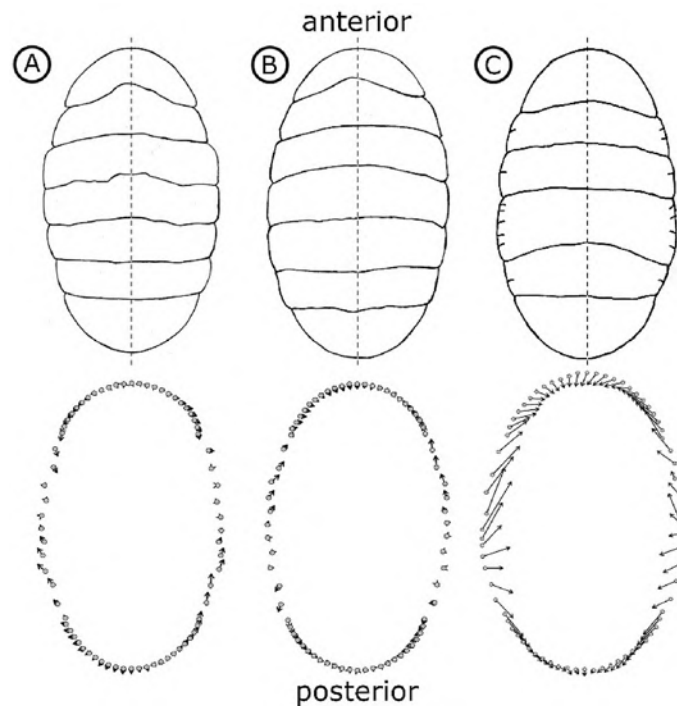


Fig. 5. Vector of change in body shape of chitons with hypomerism condition. A and B show two different chitons with seven sclerites and perfect hypomerism (HypoP); C shows a chiton with six sclerites and hypomerism with heterogeneous coalescence (HypoCo). Gray dots represent the consensus shape, and black arrows show the direction and magnitude of vectors.

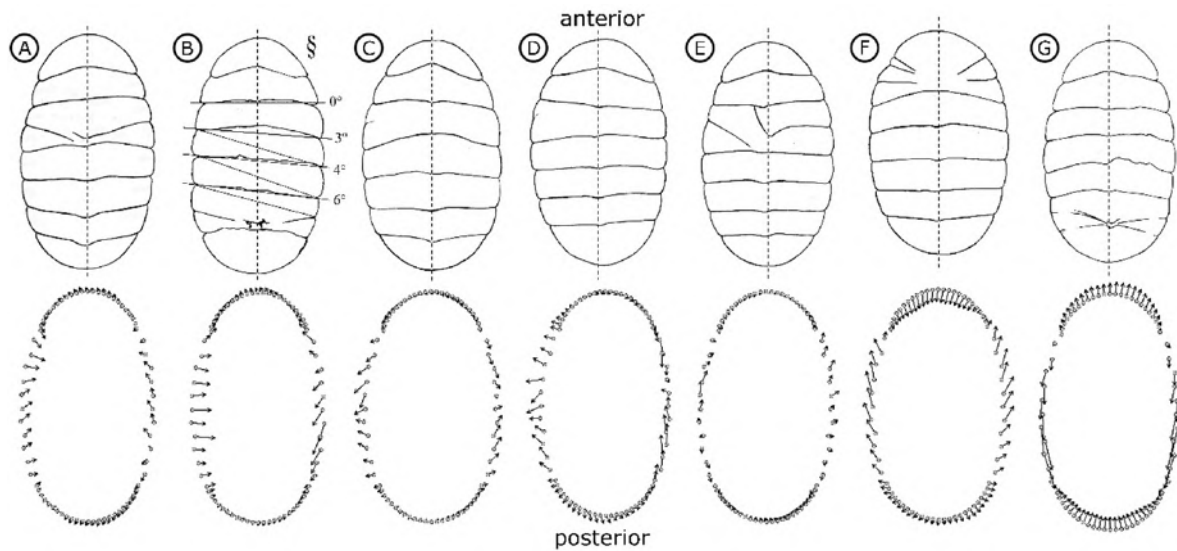


Fig. 6. Vector of change in body shape of chitons with variations of heterogeneous coalescence (HeCo) condition: A) chiton with simple HeCo condition, B) chiton with HeCo condition and a spiraled pattern, C and D) chiton with HeCo III-IV combined with hypomerism, E) chiton with HeCo III-IV combined with imperfect hypermerism, F) chiton with HeCo triple I-II-III, G) chiton with HeCo triple VI-VII-VIII. Gray dots represent the consensus shape, and black arrows show the direction and magnitude of vectors. §Abnormal chiton that may present in a malformed pattern such as helicometry, according to Scholtz (2021). The dotted line and number indicate the degree of inclination.

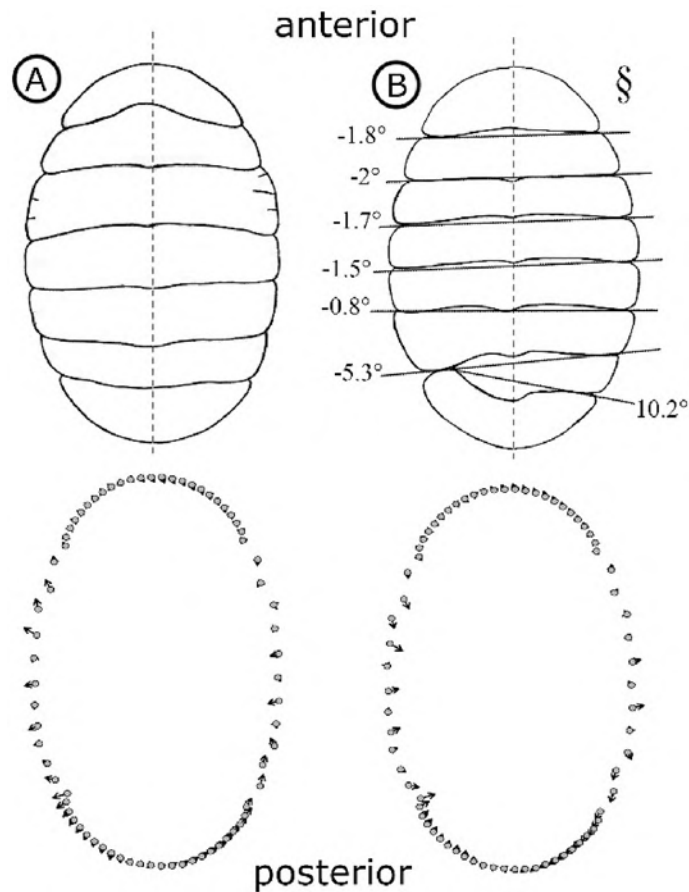


Fig. 7. Vector of change in body shape of chitons with homogeneous coalescence (HoCo) condition: A) chiton with single HoCo, B) chiton with HoCo and a spiraled pattern. Gray dots represent the consensus shape, and black arrows show the direction and magnitude of vectors. §Abnormal chiton that may present in a malformed pattern such as helicometry, according to Scholtz (2021). The dotted line and number indicate the degree of inclination.

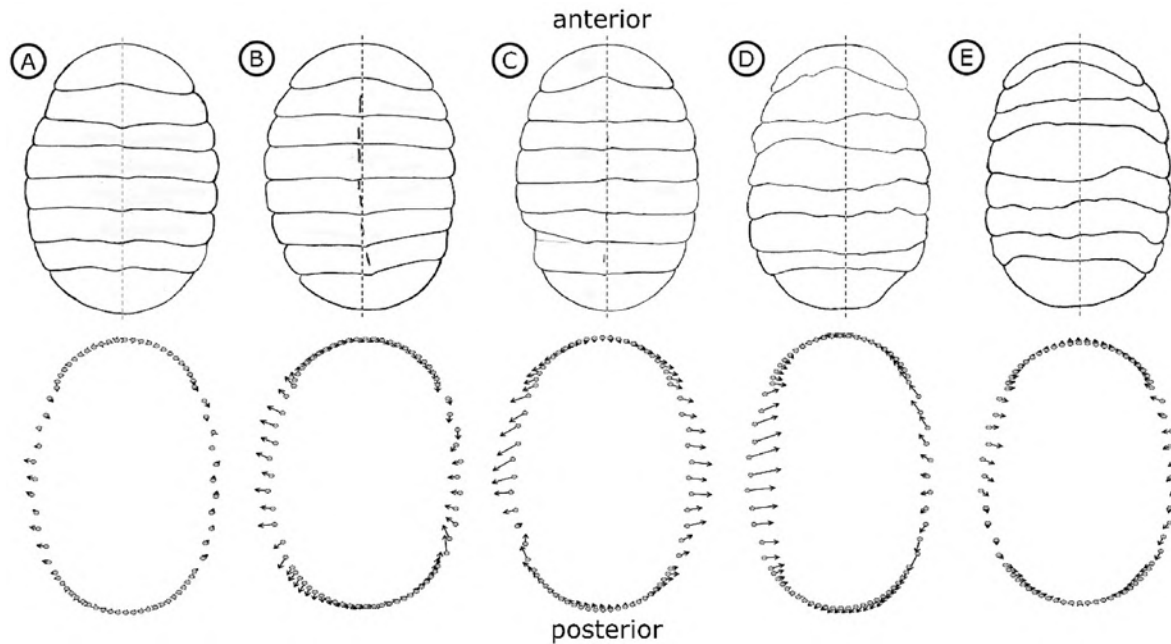


Fig. 8. Vector of change in body shape of chitons with variations of a deformed (Def) condition: A) chiton with an apparent widening of the scleritome, B) chiton with a scoliosis-like torsion, C) chiton with one side “bitten,” D and E) chitons with a hunchbacked appearance. Gray dots represent the consensus shape, and black arrows show the direction and magnitude of vectors.

1:11, 12:22), with very little change in the head (landmark 23:47) or tail (landmark 24:72).

3.3. FA expression

The bilateral symmetry test suggests that there are significant differences in FA levels between the left and right sides (Table 3). The highest variance in shape is explained by individuals (60.3%), followed by the interaction between individuals and side (14%), and a small but significant proportion of variance is explained by the side, corresponding to directional asymmetry (1.6%). The results of Procrustes ANOVA of the FA component of shape variance indicated that a non-significant percentage of variance (0.3%) is explained by the body shape condition (Table 4). These results suggest that FA levels were similar for chitons with abnormal and deformed conditions.

3.4. Direction and magnitude of the vectors that describe the shape variation of abnormal and deformed chitons

In the three chitons with hypermerism, it was observed that the fewer sclerites they presented, the greater the compression compensated with shortening; the vectors projected mainly towards the anterior part of the scleritome (Fig. 5). In chitons with a HypoP condition, the greatest change occurred in the vectors corresponding to the landmarks 8:11 (right posterior side), 12:16 (left posterior side, Figs. 5A), 1:5 (right posterior side), and 18:22 (left posterior side, Fig. 5B). The middle did not present large changes. On the contrary, the chiton with a HypoCo

condition presented changes in all vectors, which were projected towards the inside of the scleritome, giving a reduced appearance to the entire body scleritome (Fig. 5C).

In the seven chitons with a heterogeneous coalescence (HeCo) condition, a pattern of change was observed in the width and length of the body shape (Fig. 6). Those with simple and spiral HeCo conditions showed vector projections towards inside the scleritome with an anterior (Fig. 6A), a middle, and a posterior course, respectively (Fig. 6B), thus showing body-width compression. In chitons with a hypermerism HeCo condition, the vectors on the left side projected out of the body scleritome (Fig. 6C and D), showing a widening body. In the chiton with the imperfect hypermerism HeCo condition, the vectors showed little change from the consensus shape (Fig. 6E); they mostly maintained their width and length. Finally, in chitons with triple coalescence, the body shape was observed to elongate. The vectors tended to move towards the sclerites where the coalescence was (i.e., head or tail sclerites), and there was a widening compensation of the sclerites near each triple coalescence (Fig. 6F and G).

In the two chitons with homogeneous coalescence, the vectors showed little variation on the left and right sides, with an outward direction and a spiral pattern (Fig. 7). In the first case, one turn starts from the left side towards the anterior, while the second turn from the posterior goes towards the right side (Fig. 7A). In the second case, a single turn appears to start on the anterior in a rightward direction, reaching the posterior when the scleritome turns to the left side, causing a reduction in the scleritome (Fig. 7B).

For the five chitons with eight sclerites (i.e., normal) but with

Table 5

Results from the Procrustes ANOVA model to evaluate the effects of body CS, condition (abnormal and normal), and their interaction on body shape variation.

	Df	SS	MS	Rsqr	F	Z	Pr (>F)
CS	1	0.0345	0.0345	0.1166	53.3874	5.7226	0.001*
Condition	1	0.0046	0.0046	0.0157	7.199	3.2465	0.001*
CS: Condition	1	0.0031	0.0031	0.0107	4.9191	2.704	0.003*
Residuals	392	0.2536	0.0006	0.8568			
Total	395	0.2960					

**Significant effect alpha <0.01, *Significant effect alpha <0.05.

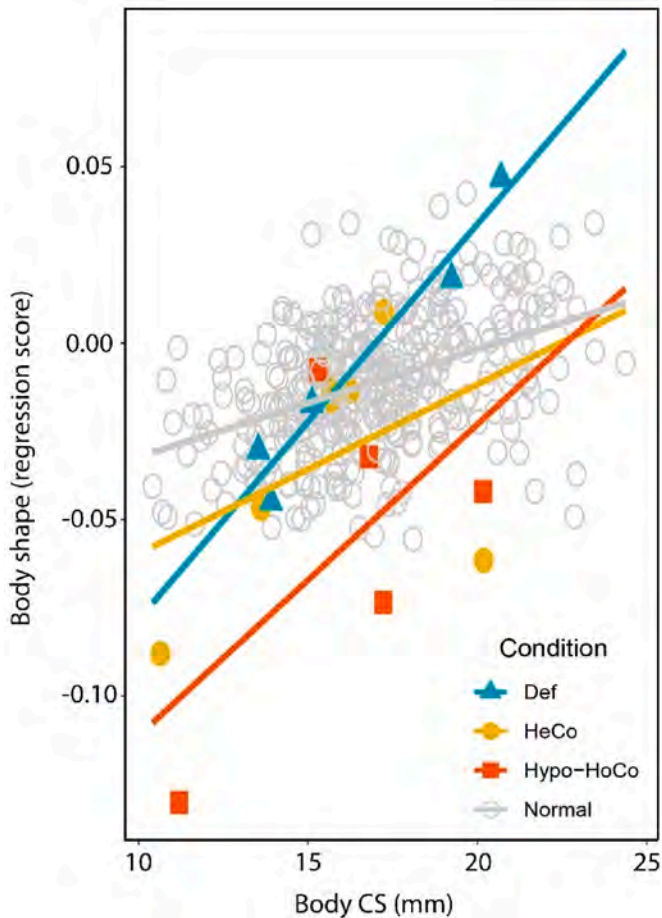


Fig. 9. Linear regression of the body shape calculated with Procrustes ANOVA on the body CS to each condition.

deformity on the body, the changes were focused on both the left and right sides, widening or compressing the body scleritome (Fig. 8). The chiton with few widenings showed some change towards the outside of

the body scleritome (Fig. 8A). In the chiton with a scoliosis-like torsion, vectors on the left side moved to the outside, while the vectors on the right side moved a little towards the inside of the scleritome (Fig. 8B). The chiton with a “bitten” side showed the greatest widening on both the left and right sides, according to the movement of the vectors (Fig. 8C). Both hunchbacked chitons showed movement of the vectors towards the inside of scleritome, but with a greater magnitude in the first case (Fig. 8D) than in the second (Fig. 8E).

3.5. Shape comparisons between abnormalities and deformities

Our results indicate that abnormal and deformed conditions did not influence variations in either size or shape. The Procrustes ANOVA model showed significant but mild effects of abnormal and deformed condition on shape variation. The greatest variation of shape is explained by the CS (11.6%), followed by condition (1.6%); the interaction between CS and condition explains 1% of the variation (Table 5). Regarding body size, the ordinary least squares (OLS) model indicated non-significant differences between normal and abnormal conditions. Results from this model showed a low and non-significant effect of abnormal conditions on CS variance of 0.56% ($F_{1,395} = 2.227, P = 0.133$).

Normal and abnormal conditions in chiton shape show a positive change direction on the regression with increments of CS. HeCo has the same trend as the normal condition, as do Def and Hypo-HoCo (Fig. 9). HypoCo showed the greatest differentiation between the different abnormalities and deformities, as well as the smallest CS (Fig. 10).

Pairwise comparisons of the consensus shapes indicated that the greatest distance (0.0509) occurred in the Hypo-HoCo condition compared to the other conditions. The normal condition showed fewer distances compared to Def and HeCo conditions. The highest probability (0.1298) was found between the normal and deformed conditions (Table 6).

4. Discussion

Landmark-based geometric morphometric studies have been widely used to measure variations in shape between individuals and populations in mollusks such as bivalves and gastropods (Valladares et al. 2010; Moneva et al. 2014; Bagaloyos et al. 2015; Abdelhady 2016; Doyle

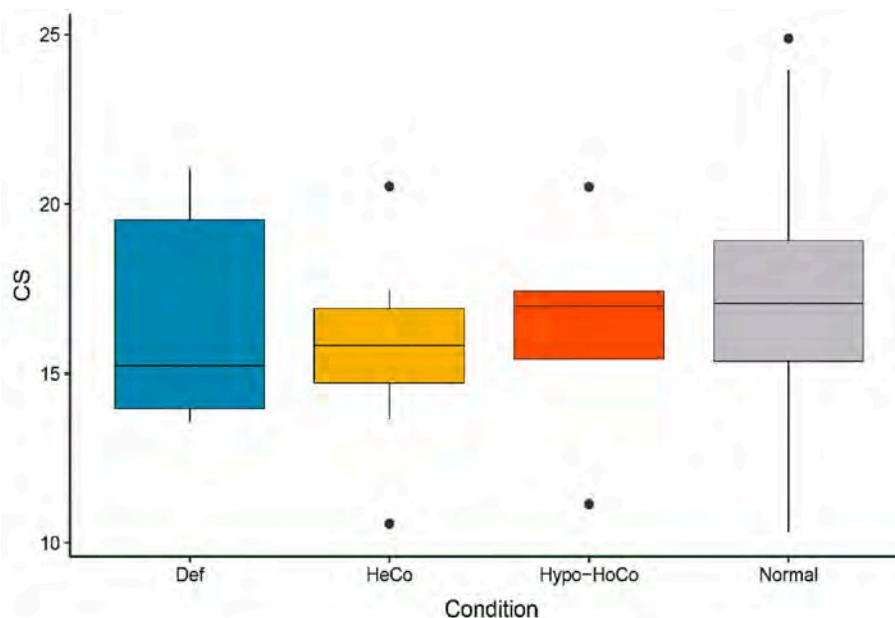


Fig. 10. Boxplots for the body centroid size of individuals with abnormalities and deformities. The line within each box represents the median, and the height of each box represents first and third quartiles (75% of all data). Lines indicate the observed minimum and maximum values, and dots are outliers.

Table 6
Results from the Pairwise comparisons (Procrustes distances) between chiton body shape conditions.

	Def	HeCo	Hypo-HoCo	Normal
Def		0.0340	0.0509	0.0186
HeCo	0.0099*		0.0307	0.0246
Hypo-HoCo	0.0009*	0.0219*		0.0424
Normal	0.1298	0.0029*	0.0009*	

Numbers in bold and grey area above the diagonal represent Procrustes distances, while numbers below the diagonal are the probabilities.

* Significant effect

et al. 2018; Ramírez-Sánchez et al. 2022). However, to our knowledge, for the class Polyplacophora, our study is the first landmark-based geometric morphometric approach to measure variations among chitons from which the mantle was removed, thus allowing the slit rays to be accessed as anatomical as reference points. While our manuscript was in the peer review process, another landmark-based geometric morphometric approach, with chitons whose mantle girdles were maintained and that used only the intersection between sclerites as anatomical points, had just been published (Hernández-P et al. 2023). Other geometric morphometric methods such as the elliptical Fourier analysis (EFA), which is a standard approach to outlining closed contours (Iwata & Ukai 2002; Sheets et al. 2006), have been used to evaluate the chiton contour while maintaining its mantle girdle (Salloum et al. 2020), since chitons are oval with closed contours that may contain valuable information about their shape.

Both landmark-based and Fourier elliptical methods are useful for quantifying morphological variation in chiton shape and determining which method to use depends on the state of the chitons to be analysed and the objectives of the study. Here, we recommend using the landmark-based protocol when the chitons are relaxed and fixed. This preserves their natural shape without bending (see Avila-Poveda's 2013 protocol) and allows the mantle to be removed without disarticulating the sclerites (valves). This, in turn, allows access to the internal part where the mantle slit rays are found and which serve as anatomical reference points, along with the intersection of the sclerites. For studies where chitons are preserved without prior relaxation and are curved, or where they belong to museum, academic, or private collections and it is impossible to remove the mantle to preserve the sample in good condition, the Fourier elliptical method may be the best option, since the outer part of the sclerites, being articulated, offers few places to put reference points that preserve the homology.

Our landmark configuration of 72 anatomical points proved to be useful in quantifying asymmetries in chiton scleritome of specimens with complex teratologic combinations, deformities, and normal conditions, since all the points can be placed in chitons that have six to eight sclerites. Although chitons with more than eight sclerites were not analysed in this study, our configuration can also be used for a hypermerism condition. In this case, we suggest placing the corresponding landmarks between the intersection of the sclerites (Fig. 3C) so that these landmarks are preserved, as slit rays may not be present in abnormal sclerites (Avila-Poveda and Ramirez-Santana, personal observation).

In general, shape change vectors in abnormal and deformed chitons showed greater variation in the anterior sclerites (sclerites I-IV), while the middle and posterior sclerites showed less variation. Therefore, the chitons acquired a wider appearance. The formation of sclerites in chitons occurs in the early stages of larval development before settlement, beginning with the simultaneous formation of sclerites II-V; then sclerites I, VI, VII; and finally, after 10 days, sclerite VIII (Kniprath 1980; Henry et al. 2004; Sirenko 2018). Given that most abnormalities in *C. articulatus* occur in sclerites III-IV, and the trajectory of the vectors

showed that shape variation is projected towards the anterior, we can deduce that during the early formation of the sclerites some process occurs that prevents the correct formation of these sclerites. Therefore, based on the vector of change in body shape of deformed and abnormal chitons compared to normal chitons, we suggest that the last sclerites are formed to compensate for any errors that may be present and thus maintain a functional oval shape. Kniprath (1980) reported that chiton larvae of the genus *Middendorffia* displayed poor plate development when exposed to temperatures above 16 °C, which prevented proper sclerite mineralization and the formation of one or more sclerites, or favoured sclerite fusion with extra indentation marks (slit rays) or unequal width.

The variation in chiton shape was mostly explained by centroid size (13%), while the different abnormalities and deformities had little impact on these variations (2%). Allometric relationships between the CS and the different conditions indicate a similar trend between them; the HeCo condition remains similar to the trend of normal chitons, while the Def and Hypo-HoCo condition trends are similar to each other, but differences in shape variance are not explained by differences in size. However, having a larger sample size within groups is necessary in order to affirm differences in allometric trends among these types of abnormalities. These results could indicate that under conditions of perfect hypomerism and hypermerism, the shape remains like that of normal chitons, but the centroid size decreases. Torres et al. (2023) suggest that chitons with abnormalities are similar in size and shape to normal chitons of the same species. Avila-Poveda et al. (2019) reported that the coalescence condition was found most frequently and to different degrees, generating various combinations with other abnormalities, which suggests that coalescence was an intermediate step towards perfect hypo- or hypermerism. The similar trend we found between HeCo and normal regression could suggest that HeCo is an intermediate step towards a normal condition.

Although chitons with abnormal and deformed conditions showed a small but significant proportion of variance in the left and right sides (1.6%), the bilateral symmetry test revealed the oval shape was visually maintained on both sides of the body. Bilateral animals such as mollusks possess genes that control the formation of the anteroposterior axis of the body; these are called Hox and ParaHox genes (Finnerty et al. 2004; Aronowicz & Lowe 2006; Barucca et al. 2006). In the classes Bivalvia, Gastropoda and Cephalopoda, the Hox and ParaHox genes also play a crucial role in the development of the shell and specific organs such as the foot and tentacles (Barucca et al. 2006; Biscotti et al. 2007).

In the class Polyplacophora, the Hox and ParaHox genes define a flat anteroposterior axis that allows the subsequent formation of sclerites (Fritsch et al. 2015; 2016), specifically a group of *engrailed* genes that are responsible for body segmentation (Jacobs et al. 2000). We hypothesize that at this early stage of larval development, one or more *engrailed* genes are not expressed correctly and this causes the axis to present malformations that later produce abnormalities in the ontogeny of the sclerites, which may then result in an abnormal biomineralization processes. However, as much is still unknown about gene expression

patterns in developing chitons, this remains as a research question. Regarding the possible helicotomy pattern present in some specimens of *C. articulatus* according to Scholtz (2021), it could be a type of fluctuating helical asymmetry, such as that which occurs in snails with equiangular spiral shells that have been exposed to pesticides or ammonia emissions or have some degree of erosion on their shells (Graham et al. 2010). Asymmetries in chiton scleritome have been found in the genus *Cryptochiton*, but these are caused by constant shell repair processes due to sclerite injuries that are flat, very thin, and constitute only 7.4% of body weight and not because of a teratology (Tucker & Giese 1959).

Similarly, no effect was detected from abnormalities on CS variance. Size differences among individuals could be explained by other factors. These results corroborate the idea of constant shell repair processes (Tucker & Giese 1959) that ensure the performance of individuals in their natural environments.

The low levels of FA expressed in *C. articulatus* indicate that although this species lives in areas of high stress, such as the rocky intertidal shore, it maintains stability in its development. Ducos & Tabugo (2015) found high levels of FA in the intertidal bivalve *Gafrarium tumidum* collected from three locations in the Philippines; thus, the shell has considerable variations in shape. The authors identify pollution and the deterioration of the habitat as the main sources of stress.

Declaration of competing interest

The authors declare the following financial interests/personal relationships which may be considered as potential competing interests: Omar Hernando Avila-Poveda reports financial support was provided by Consejo Nacional de Humanidades, Ciencias y Tecnologías (CONAHCYT). Omar Hernando Avila-Poveda reports financial support was provided by Universidad Autónoma de Sinaloa (UAS).

Data availability

Data will be made available on request.

Acknowledgments

This research took place within the frame of the large-scale project “Quitón del Pacífico tropical mexicano®,” led by Avila-Poveda OH. Ramirez-Santana BP received a CONAHCYT scholarship, and the results presented here are part of her Ph.D. dissertation in the Posgrado en Ciencias en Recursos Acuáticos, FACIMAR-UAS. This research was funded by PROFAPI-UAS projects 2014/023 and PRO/2022_A7_002 and the grants from SNI-CONAHCYT and CATEDRA-CONAHCYT awarded to O.H. Avila-Poveda. Specimen collection was done under research permits (PPF/DGOPA-130/15 and PPF/DGOPA-110/21) granted to O.H. Avila-Poveda by SAGARPA (currently *Secretaría de Agricultura y Desarrollo Rural* “SADER”) through *Comisión Nacional de Acuicultura y Pesca* “CONAPESCA.” The authors extend special thanks to more than 50 volunteers and social services and Research Residency students who helped with fieldwork in each sampling and in the laboratory. Ospina-Garcés SM is supported by a postdoctoral fellowship from CONAHCYT, Avila-Poveda OH is a CONAHCYT Research Fellow hosted by the Facultad de Ciencias del Mar “FACIMAR,” Universidad Autónoma de Sinaloa “UAS” (project no. 2137) in the research group “Manejo de Recursos Pesqueros UAS-CA-132, UAS-FACIMAR”. We are grateful to an anonymous reviewer for helpful comments and special thanks to non-anonymous reviewer Douglas J. Erniste for his extensive and valuable suggestions and comments, which have greatly improved the quality of this manuscript.

Appendix A. Supplementary data

Supplementary data to this article can be found online at <https://doi.org/10.1016/j.jcz.2023.06.008>.

References

- Abadia-Chanona, Q.Y., Avila-Poveda, O.H., Arellano-Martinez, M., Ceballos-Vazquez, B. P., 2016. Observation and establishment of gonad development stages in polyplacophorans (Mollusca): *Chiton (Chiton) articulatus* a case study. *Acta Zool.* 97, 506–521.
- Abdelhady, A.A., 2016. Phenotypic differentiation of the Red Sea gastropods in response to the environmental deterioration: geometric morphometric approach. *J. Afr. Earth Sci.* 115, 191–202.
- Adams, D.C., Otárola-Castillo, E., 2013. Geomorph: an R package for the collection and analysis of geometric morphometric shape data. *Methods Ecol. Evol.* 4, 393–399.
- Adams, D.C., Rohlf, F.J., Slice, D.E., 2004. Geometric morphometrics: ten years of progress following the ‘revolution’. *Ital. J. Zool.* 71, 5–16.
- Adams, D.C., Collyer, M.L., Kaliontzopoulou, A., 2019. Geomorph: Software for Geometric Morphometric Analyses. R package version 3.1.0. <https://cran.r-project.org/package=geomorph>.
- Anderson, D.T., 2001. *Invertebrate Zoology*, second ed. Oxford University Press, South Melbourne, Australia, p. 467.
- Anseu, B., Terryn, Y., 2003. Intertidal chitons (Mollusca: Polyplacophora) from the coast of Jordan, red sea, with the description of a new species of *Parachiton* Thiele, 1909. *Bollettino Malacologico* 39, 1–24.
- Aronowicz, J., Lowe, C.J., 2006. Hox gene expression in the hemichordate *Saccoglossus kowalevskii* and the evolution of deuterostome nervous systems. *Integr. Comp. Biol.* 46, 890–901.
- Avila-Poveda, O.H., 2013. Annual change in morphometry and in somatic and reproductive indices of *Chiton articulatus* adults (Polyplacophora: Chitonidae from Oaxaca, Mexican Pacific. *Am. Malacol. Bull.* 31, 65–74.
- Avila-Poveda, O.H., 2020. Large-scale project ‘Chiton of the Mexican tropical pacific’: *Chiton articulatus* (Mollusca: Polyplacophora). *Res. Ideas and Outcomes* 6, e60446.
- Avila-Poveda, O.H., Ramirez-Santana, B.P., Martinez-Diaz, P., Ramirez-Perez, J.S., Saavedra-Sotelo, N.C., Vargas-Trejo, B., Amezcua-Gomez, C.A., Melendez-Galicia, C., 2019. Complex abnormality combinations between the scleritome and the sclerites of *Chiton articulatus* (Mollusca: Polyplacophora): new findings for the teratological classification. *Zool. Anz.* 279, 68–81.
- Avila-Poveda, O.H., Rodriguez-Dominguez, G., Ramirez-Perez, J.S., Perez-González, R., 2020. Plasticity in growth parameters of an intertidal rocky shore chiton (Polyplacophora: chitonida) under pre-ENSO and ENSO events. *J. Molluscan Stud.* 86, 72–78.
- Bagaloyos, J.B., Manting, M.M.E., Gorospe, J.G., Demayo, C.G., 2015. Geometric morphometric description of the shell shapes in juvenile spider conch *Lambis lambis*. *Adv. Environ. Biol.* 9, 164–170.
- Barucca, M., Biscotti, M.A., Olmo, E., Canapa, A., 2006. All the three ParaHox genes are present in *Nuttallochiton mirandus* (Mollusca: Polyplacophora): evolutionary considerations. *J. Exp. Zool.* 306B, 164–167.
- Baschieri, L., Dell’Angelo, B., Palazzi, S., 1992. Recenti ritrovamenti di Polyplacophora anomala nel Mediterraneo. *Boll. Malacol.* 28, 65–68 [in Italian].
- Benítez, H.A., Lemic, D., Villalobos-Leiva, A., Bažok, R., Órdenes-Claveria, R., Živković, I. P., Mikac, K.M., 2020. Breaking symmetry: fluctuating asymmetry and geometric morphometrics as tools for evaluating developmental instability under diverse agroecosystems. *Symmetry* 12, e1789.
- Berry, S.S., 1935. A further record of a *Chiton* (Nuttallina) with nine valves. *Nautilus* 48, 89–90.
- Biscotti, M.A., Canapa, A., Olmo, E., Barucca, M., 2007. Hox genes in the antarctic polyplacophoran *nuttallochiton mirandus*. *Journal of experimental zoology (MOL DEV EVOL)*. In: 308B: 507–513. Bookstein F.L. 1997. *Morphometric Tools for Landmark Data: Geometry and Biology*. Cambridge University Press, Cambridge, United Kingdom, p. 435.
- Bookstein, F.L., 1996. In: Mardia, K.V., Gill, C.A. (Eds.), *Applying Landmark Methods to Biological Outline Data. Image Fusion and Shape Variability*, Dryden IL. University of Leeds Press, Leeds, United Kingdom, pp. 79–87.
- Brusca, R.C., Brusca, G.J., 2005. *Invertebrados 1ra Edición*. McGraw-Hill Interamericana, Madrid, España, p. 1032 [p in Spanish].
- Bullock, R.C., 1988. The Genus *Chiton* in the new world (Polyplacophora: Chitonidae). *Veliger* 31, 141–191.
- Burghardt, G., Burghardt, L., 1969. Report on some abnormal chitons from California and British Columbia. *Veliger* 12, 228–229.
- Chace, E.P., Chace, E.M., 1930. Two seven-valved chitons from Mendocino, California. *Nautilus* 44, 7–8.
- Collyer, M.L., Adams, D.C., 2018. RRPP: An r package for fitting linear models to high-dimensional data using residual randomization. *Methods Ecol. Evol.* 9, 1772–1779.
- Collyer, M.L., Adams, D.C., 2019. RRPP: Linear Model Evaluation with Randomized Residuals in a Permutation Procedure. R Package Version 0.4.0. <https://CRAN.R-project.org/package=RRPP>.
- Crozier, W.J., 1919. Coalescence of the shell-plates in *Chiton*. *Am. Nat.* 53, 278–279.
- Dell’Angelo, B., 1982. Sui casi di anomalie nel numero di piastre dei Polyplacophora. *Bollettino Malacologico* 18, 235–246 [In Italian].
- Dell’Angelo, B., Cianfanelli, S., 2002. Una nuova segnalazione di ipermeria nei molluschi poliplacefori. *Atti della Società Toscana di Scienze Naturali – Memorie serie B* 129, 27–28 [In Italian].
- Dell’Angelo, B., Schwabe, E., 2010. Teratology in chitons (Mollusca, Polyplacophora): a brief summary. *Bollettino Malacologico* 46, 9–15.
- Dell’Angelo, B., Palazzi, S., 1983. Recenti ritrovamenti di Polyplacophora anomala in Sardegna. *Boll. Malacol.* 19, 253–256 [in Italian].
- Dongen, S.V., 2006. Fluctuating asymmetry and developmental instability in evolutionary biology: past, present and future. *J. Evol. Biol.* 19, 1727–1743.

- Doyle, D., Gammell, M.P., Nash, R., 2018. Morphometric methods for the analysis and classification of gastropods: a comparison using *Littorina littorea*. *J. Molluscan Stud.* 84, 190–197.
- Doyle, D., Frias, J., Gammell, M.P., Lynch, M., Nash, R., 2022. Assessing the morphological impacts of long-term harvesting in intertidal gastropods using historical data and morphometric tools. *J. Molluscan Stud.* 88, eyac019.
- Ducos, M.B., Tabugo, S.R.M., 2015. Fluctuating asymmetry as bioindicator of stress and developmental instability in *Gafrarium tumidum* (ribbed venus clam) from coastal areas of Iligan Bay, Mindanao, Philippines. *Aquaculture, Aquarium, Conserv. Legis. Int. J. Bioflux Soc.* 8, 292–300.
- Dunithan, A., Jacquemin, S., Pyron, M., 2012. Morphology of *Elimia livescens* (Mollusca: pleuroceridae) in Indiana, USA covaries with environmental variation. *Am. Malacol. Bull.* 30, 127–133.
- Ferreira, A.J., 1983. The chiton fauna of the revillagigedo archipelago, Mexico. *Veliger* 25, 307–322.
- Finnerty, J.R., Pang, K., Burton, P., Paulson, D., Martindale, M.Q., 2004. Origins of bilateral symmetry Hox and dpp expression in a sea anemone. *Science* 304, 1335–1337.
- Fritsch, M., Wollesen, T., de Oliveira, A.L., Wanninger, A., 2015. Unexpected co-linearity of Hox gene expression in an aculiferan mollusk. *BMC Evol. Biol.* 15, e151.
- Fritsch, M., Wollesen, T., Wanninger, A., 2016. Hox and ParaHox gene expression in early body plan patterning of polyplacophoran mollusks. *J. Exp. Biol.* 326, 89–104.
- Graham, J.H., Raz, S., Hel-Or, H., Nevo, E., 2010. Fluctuating asymmetry: methods, theory, and applications. *Symmetry* 2, 466–540.
- Guillén, C., Urteaga, D., 2019. First records of coalescence and hypomerism in *Tonicia atrata* (Polyplacophora, chitonidae) in the southwestern atlantic ocean. *Revista del Museo Argentino de Ciencias Naturales* 21, 1–6.
- Gunz, P., Mitteroecker, P., 2013. Semilandmarks: a method for quantifying curves and surfaces. *Hystrix* 24, 103–109.
- Gutiérrez-Cabrera, A.E., Badillo Montaño, R., González, L., Ospina-Garcés, S.M., Córdoba-Aguilar, A., 2022. Body shape and fluctuating asymmetry following different feeding sources and feeding time in a triatomine, *Triatoma pallidipennis* (Stål, 1892). *Infect. Genet. Evol.* 98, e105199.
- Henry, J.Q., Okusu, A., Martindale, M.Q., 2004. The cell lineage of the polyplacophoran, *Chaetopleura apiculata*: variation in the spiralian program and implications for molluscan evolution. *Dev. Biol.* 272, 145–160.
- Hernández-P, R., Benítez, H.A., Ornelas-García, C.P., Correa, M., Suazo, M.J., Piñero, D., 2023. Bergmann's rule under rocks: testing the influence of latitude and temperature on a chiton from Mexican marine ecoregions. *Biology* 12, e766.
- Holló, G., 2015. A new paradigm for animal symmetry. *Interface Focus* 5, e20150032.
- Ibañez, C.M., Sepulveda, R.D., Sigwart, J.D., 2018. Comparative allometric variation in intertidal chitons (Polyplacophora: chitonidae). *Zoomorphology* 137, 249–256.
- Iredale, T., Hull, B., 1925. A monograph of the Australian Loricates. *Aust. Zool.* 4, 256–276.
- Iwata, H., Ukai, Y., 2002. SHAPE: a computer program package for quantitative evaluation of biological shapes based on elliptic Fourier descriptors. *J. Hered.* 93, 384–385.
- Jacobs, D.K., Wray, C.G., Wedeen, C.J., Kostriken, R., DeSalle, R., Staton, J.L., Gates, R. D., Lindberg, D.R., 2000. Molluscan engrailed expression, serial organization, and shell evolution. *Evol. Dev.* 2, 340–347.
- Kaas, P., Van Belle, R.A., 1981. The genus *lepidochitona* gray, 1821 (Mollusca: Polyplacophora) in the northeastern atlantic ocean, the mediterranean sea and the black sea. *Zool. Verhandl.* 185, 3–43.
- Kingston, A.C.N., Sigwart, J.D., Chappell, D.R., 2020. Monster or multiplacophoran: a teratological specimen of the chiton *Acanthopleura granulata* (Mollusca: Polyplacophora) with a valve split into independent and symmetrical halves. *Acta Zool.* 101, 242–246.
- Klingenberg, C.P., 2015. Analyzing fluctuating asymmetry with geometric morphometrics: concepts, methods, and applications. *Symmetry* 7, 843–934.
- Klingenberg, C.P., 2022. Shape asymmetry: what's new? *Emerg. Topics in Life Sci.* 6, 285–294.
- Kniprath, E., 1980. Ontogenetic plate and plate field development in two chitons, *Middendorffia* and *Ischnochiton*. *Wilhelm Roux's Archive* 189, 97–106 ([Continued as *Development Genes and Evolution*]).
- Kocot, K.M., Aguilera, F., McDougall, C., Jackson, D.J., Degnan, B.M., 2016. Seashell diversity and rapidly evolving secretomes: insights into the evolution of biomineralization. *Front. Zool.* 13, 13–23.
- Kuhl, F.P., Giardina, C.R., 1982. Elliptic fourier features of a closed contour. *Comput. Graph. Image Process* 18, 236–258 [Continued as *Graph. Models*].
- Langer, P.D., 1978. Abnormality of shell plates in three chitons from New England. *Veliger* 21, 274–275.
- Manuel, M., 2009. Early evolution of symmetry and polarity in metazoan body plans. *Comptes Rendus Biol.* 332, 184–209.
- Moreno, C.S.O., Baquiano, P.M.L., Blasco Jr., J.O., Borlaza, K.M.E., Burias, D.M.E., Flores, K.A., Fuentes, G.R.E., Pancho, A.G.E., Sanchez, R.R.G., 2014. Comparative morphological descriptions of interior shell patterns of the Venerid bivalves: *Meretrix lyrata*, *Mercenaria mercenaria* and *Venerupis philippinarum* using Landmark-based Geometric Morphometric Analysis. *Aquaculture, Aquarium, Conservation & Legislation International Journal of the Bioflux Society* 7, 386–395.
- Palmer, R., 1994. Fluctuating asymmetry analyses: a primer. In: Markow, T.A. (Ed.), *Developmental Instability: its Origins and Evolutionary Implications*, Contemporary Issues in Genetics and Evolution, vol. 2. Springer, Netherlands, pp. 335–364.
- Pelseener, P., 1919. La metamérie et l'hypermérie chez les chitons. *Annales de la Société Royale Zoologique et Malacologique de Belgique* 50, 41–43 ([In French]).
- Poutiers, J.M., 1995. Quitones (Anfineuros, loricados, polioplacóforos). In: Fischer, W., Krupp, F., Schneider, W., Sommer, C., Carpenter, K.E., Niem, V.H. (Eds.), *Guía FAO para la identificación de especies para los fines de la pesca. Pacífico Centro-Oriental: Plantas e Invertebrados*, vol. 1. FAO, Roma, pp. 299–304.
- Prelle, G., Sosso, M., Dell'Angelo, B., 2013. Variabilità cromatica ed ipomeria in due specie di chitoni (Polyplacophora) del Madagascar meridionale. *Bollettino Malacologico* 49, 12–17 ([In Italian]).
- Quintana, H.L., Hernández, J., 2021. Abundance and morphometry of chitons (Mollusca: Polyplacophora) associated with breakwaters in Coveñas, Sucre-Colombia. *Intropica* 16, 55–65.
- R Core Team, 2017. *In: R: A Language and Environment for Statistical Computing*. R Foundation for Statistical Computing, Vienna, Austria. <https://www.R-project.org/>.
- Ramírez-Sánchez, M.M., Ávila-Valle, Z.A., Ospina-Garcés, S.M., Saito-Quezada, V.M., Salgado-Ugarte, I.H., 2022. A geometric morphometric reappraisal of the shell morphology during growth in the pearl oyster *Pinctada mazatlanica*. *Biología* 77, 2875–2886.
- Rohlf, F.J., 2017. Tpsdig, Version 2.3, tpsUtil Version 1.74. Department of Ecology and Evolution, Stony Brook.
- Rohlf, F.J., Slice, D., 1990. Extensions of the Procrustes method for the Optimal superimposition of landmarks. *Syst. Zool.* 39, 40–59.
- Roth, B., 1966. Some abnormal chitons from Washington State. *Veliger* 9, 249–250.
- Ruppert, E.E., Barnes, R.D., 1996. *Zoología de los invertebrados* 6ta edición. McGraw-Hill Interamericana. Cd. de México, México. ([In Spanish]).
- Salloum, P.M., De Villemereuil, P., Santure, A.W., Waters, J.M., Lavery, S.D., 2020. Hitchhiking consequences for genetic and morphological patterns: the influence of kelp-raffing on a brooding chiton. *Biol. J. Linn. Soc.* 130, 756–770.
- Salloum, P.M., Lavery, S.D., De Villemereuil, P., Santure, A.W., 2023. Local adaptation in shell shape traits of a brooding chiton with strong population genomic differentiation. *Evolution* 77, 210–220.
- Sampedro-M, A.C., Prasca-S, S.M., Suárez-V, D., Escobar-S, L., 2012. Estado de las poblaciones de quitones (Mollusca: Polyplacophora) en rompeolas artificiales de Coveñas, Sucre, Colombia. *Caldasia* 34, 397–407 [in Spanish].
- Savriama, Y., 2018. A step-by-step guide for geometric morphometrics of floral symmetry. *Front. Plant Sci.* 9, e1433.
- Scalici, M., Traversetti, L., Spani, F., Malafoglia, V., Colamartino, M., Persichini, T., Cappello, S., Mancini, G., Guerriero, G., Colasanti, M., 2017. Shell fluctuating asymmetry in the sea-dwelling benthic bivalve *Mytilus galloprovincialis* (Lamarck, 1819) as morphological markers to detect environmental chemical contamination. *Ecotoxicology* 26, 396–404.
- Scholtz, G., 2021. Screwed up: spirality of segments and other iterated structures suggest an underlying principle of seriality in bilaterians. *J. Morphol.* 282, 833–846.
- Schwabe, E., 2010. Illustrated summary of chiton terminology. *Spixiana* 33, 171–194.
- Sheets, H.D., Covino, K.M., Panasiewicz, J.M., Morris, S.R., 2006. Comparison of geometric morphometric outline methods in the discrimination of age-related differences in feather shape. *Front. Zool.* 3, 1–15.
- Sigwart, J.D., Andersen, S.B., Schnetler, K.I., 2007. First record of a chiton from the Palaeocene of Denmark (Polyplacophora: leptoichitonidae) and its phylogenetic affinities. *J. Syst. Palaeontol.* 5, 123–132.
- Sirenko, B.I., 2018. The larval development of the Chiton *Deshayesiella curvata* (Carpenter in dall, 1879) (Mollusca: Polyplacophora). *Russ. J. Mar. Biol.* 44, 304–308.
- Sirenko, B.I., Ibañez, C.M., 2023. Comparative morphology of *tonicia* (Polyplacophora) geographical ecotypes from southeastern pacific. *Ruthenica* 33, 27–45.
- Taki, I., 1932. On some cases of abnormality of the shell-plates in chitons. *Memoirs College Sci.* 8, 27–64. Kyoto Imperial University, Serie B.
- Tamburi, N.E., Martín, P.R., 2013. Allometric and trophic effects on shell morphology of *Pomacea canaliculata* (Caenogastropoda, Ampullariidae) from a geometric morphometrics viewpoint. *Molluscan Res.* 33, 223–229.
- Teso, V., Signorelli, J.H., Pastorin, G., 2011. Shell phenotypic variation in the southwestern Atlantic gastropod *Olivancillaria carcellesi* (Mollusca: olividae). *J. Mar. Biol. Assoc. U. K.* 91, 1089–1094.
- Torres, F.I., Ibañez, C.M., Sanhueza, V.E., Pardo-Gandarillas, M.C., 2018. Mollusk freaks: new teratological cases on marine mollusks from the South Pacific Ocean. *Latino Am. J. Aquat. Res.* 46, 683–689.
- Torres, F.I., Gálvez-Herrera, O., Ibañez, C.M., 2023. Morphometrics of teratological specimens from two species of *plaxiphora* (Mollusca, Polyplacophora) from the south pacific ocean. *Zoomorphology*, es00435-023-00607-6.
- Tucker, J.S., Giese, A.C., 1959. Shell repair in chitons. *Biol. Bull.* 116, 318–322.
- Valladares, A., Manríquez, G., Suárez-Isla, B.A., 2010. Shell shape variation in populations of *Mytilus chilensis* (Hupe 1854) from southern Chile: a geometric morphometric approach. *Mar. Biol.* 157, 2731–2738.
- Yuvero, M.C., Giménez, J., 2021. Morphological shell characterization of *Fissurellidea* and *Fissurella* (Vetigastropoda: fissurellidae) along the Argentinean coast, from temperate to subantarctic waters. *Polar Biol.* 44, 1903–1909.
- Zelditch, M.L., Swiderski, D.L., 2021. *Geometric Morphometrics for Biologists: A Primer* (3rd Edition). Elsevier Academic Press, San Diego, California, USA.

Supplementary material: <https://doi.org/10.1016/j.jcz.2023.06.008>

A landmark-based geometric morphometric approach to quantify deviations from bilateral symmetry in Polyplacophorans

Brenda Paola Ramirez-Santana ^{a, b}, Sandra Milena Ospina-Garcés ^{c, d, *}, Jorge Saul Ramirez-Perez ^a, Omar Hernando Avila-Poveda ^{a, b, e, **}

a Facultad de Ciencias del Mar (FACIMAR), Universidad Autónoma de Sinaloa (UAS), Mazatlán, Sinaloa, México

b Proyecto Quitón del Pacífico tropical mexicano. Mazatlán, Sinaloa, México

c Centro de Investigación en Biodiversidad y Conservación (CIByC), Universidad Autónoma del Estado de Morelos, Cuernavaca, Morelos, México

d Centro de Investigaciones Tropicales (CITRO), Universidad Veracruzana (UV), Xalapa, Veracruz, México

e Programa de Investigadoras e Investigadores por México, Consejo Nacional de Humanidades, Ciencias y Tecnologías (CONAHCYT), Ciudad de México, México

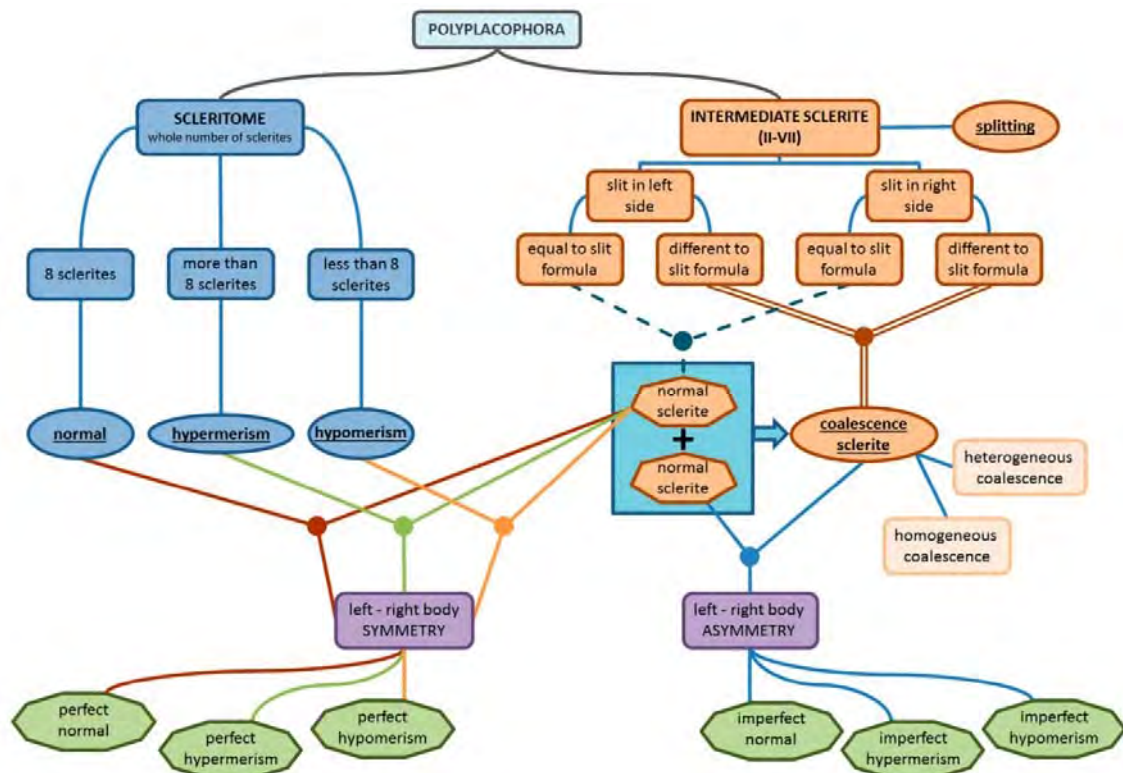


Figure S1. Guide for teratological diagnosis in Polyplacophora. The underlined names refer to abnormality types previously established in the literature.